PHYSICAL REVIEW APPLIED **22,** 024037 (2024)

Conditions for enhanced shot noise in field-effect transistors

Fabrizio Mazziotti,[1,*] Demetrio Logoteta,[2,†] and Giuseppe Iannaccone[1,‡]

[1] *Dipartimento di Ingegneria dell'Informazione, Università di Pisa, Via Caruso 16, Pisa 56122, Italy*
[2] *Dipartimento di Ingegneria dell'Informazione, Elettronica e Telecomunicazioni, Università di Roma La Sapienza, via Eudossiana 18, Roma 00184, Italy*

(Received 29 May 2024; accepted 18 July 2024; published 12 August 2024)

We demonstrate that it is possible to observe enhanced shot noise in field-effect transistors, i.e., a current noise spectral density $S > S_{\mathrm{Poisson}}$, where $S_{\mathrm{Poisson}} = 2qI$ is the so-called "shot noise" spectral density associated to a Poissonian process of electrons traversing the channel. Whereas the effects responsible for shot-noise suppression have been broadly investigated, here we unveil the mechanism and the conditions leading to an enhancement of shot noise in field-effect transistors biased in the subthreshold or weak inversion regime, that have particular relevance in the case of short-channel metal-oxide-semiconductor field-effect transistors. The effect is due to the interplay between carrier backscattering in the channel and Coulomb repulsion among carriers. We evaluate quantitatively the effect with a semianalytical model for different types of transistors, and find a characteristic shape of the Fano factor $F = S/S_{\mathrm{Poisson}}$ as a function of gate bias, that enables us to look for the signature of this effect in experiments.

DOI: 10.1103/PhysRevApplied.22.024037

I. INTRODUCTION

The distinctive character of semiconductor technology is the relentless miniaturization of transistors and the exponential increase of their integration density. This implies that transistors are operated at progressively lower voltages and currents, enabling the use of low-power electronic systems in mobile, wearable, and implantable applications. It also implies an increasing impact of noise on circuit performance and a higher sensitivity of noise behavior to localized phenomena causing fluctuations, such as single-electron trapping [1].

Indeed, the so-called shot noise—associated to the random fluctuations of the current flow due to the discrete nature of charge—is a rich source of information on electron-electron interaction, and therefore has attracted the interest of scientists in the field of mesoscopic physics [2–6] in silicon transistors [7–11] and in carbon-based electron devices [12–16].

Shot noise is one of the main noise sources in short-channel field-effect transistors (FETs) [8,17–19], as it is produced as carriers cross the potential barrier in the channel in their path from source to drain. If carriers do not interact with each other, barrier crossings are not correlated and their collective behavior can be described by a Poissonian process: in this case and if crossings are practically only in one direction (e.g., from source to drain), the current noise spectral density S is equal to $S_{\mathrm{Poisson}} = 2qI$, where I is the average channel current and q is the elementary charge. If we reduce the drain-to-source voltage approaching an equilibrium condition, crossings become bidirectional and the current-noise spectral density approaches the thermal noise $S_{\mathrm{thermal}} = 4kTG$, where k is Boltzmann's constant, T is the absolute temperature, and G is the channel conductance at equilibrium. This is also the reason why shot noise is more relevant for short-channel transistors, where longitudinal electric fields tend to be typically higher and crossings are essentially unidirectional through the potential barrier close to the source.

Deviations from a Poissonian shot noise can occur if correlations are introduced in carrier channel crossings, for example, because of electrostatic forces among carriers or because of Pauli exclusion principle. Both phenomena can be influenced by scattering events in the channel.

For this reason, shot noise is a key source of information of electron-electron correlations in semiconductor devices. The relevant figure of merit in this case is the so-called Fano factor, F, which is defined as

$$F = \frac{S}{S_{\mathrm{Poisson}}} = \frac{S}{2qI}. \tag{1}$$

If $F < 1$ we have *suppressed* or *sub-Poissonian* shot noise, meaning that carrier crossings are negatively correlated so that we have an antibunching behavior. Shot noise suppression was theoretically predicted and experimentally

---

[*] Contact author: f.mazziotti1@phd.unipi.it, fabrymazziotti@gmail.com
[†] Contact author: demetrio.logoteta@uniroma1.it
[‡] Contact author: giuseppe.iannaccone@unipi.it

reported in a variety of electron devices and mesoscopic structures [2–6,8–17,20–22].

If $F > 1$ we have *enhanced* or *super-Poissonian* shot noise, meaning that carrier crossings are positively correlated, i.e., we have carrier bunching. Shot-noise enhancement was predicted and experimentally verified as a result of the interplay between electrostatic repulsion and the particular shape of the density of states in resonant tunneling diodes biased in the negative differential resistance region [2,3,20,21] and predicted in field-effect transistors in the presence of band-to-band tunneling [12].

Here, we present another mechanism for the enhancement of shot noise in general (thermionic) field-effect transistors, as a consequence of the interplay between electron-electron Coulomb repulsion and of electron scattering in the channel. Such a mechanism occurs when FETs are biased in subthreshold or in weak inversion, and can be particularly evident in short-channel transistors, where transport is determined by the potential barrier near the source, and in the case of low contact resistance.

In the next section, we briefly discuss our device model, considering a thin-film transistor, without loss of generality. In Sec. III we present our shot noise model and discuss the different contributions leading to shot-noise enhancement and suppression. In Sec. IV we analyze the dependence of the Fano factor on the physical transistor parameters, in Sec. V we examine the case of a silicon metal-oxide-semiconductor FET and in Sec. VI we draw our conclusion. We report the derivation details in the Appendix.

II. TRANSISTOR MODEL

The considered thin-film transistor structure is illustrated in Fig. 1. A film of thickness t_{ch} and width W, deposited on an insulating substrate, acts as the transistor body, containing the channel. A top gate of length L_{G} is capacitively coupled to the channel through an insulator of thickness t_{ox} and relative dielectric permittivity ϵ_{ox}, and modulates the height of the potential barrier in the channel and therefore the current between drain and source. The transport direction is denoted by x, while the confinement direction of channel film is denoted by y. The transistor model is described in detail in Ref. [23]. Here we briefly described it and for simplicity we only take into account the lowest two-dimensional subband induced by the vertical confinement of the film. Only small quantitative deviations are obtained if we include a larger number of subbands [23,24].

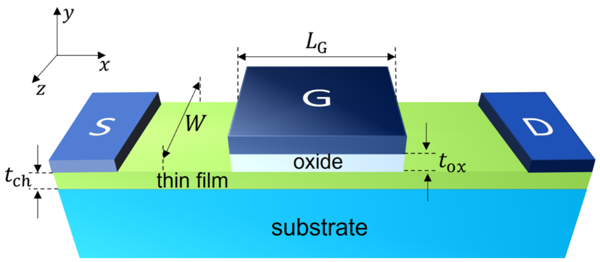

FIG. 1. Illustration of the considered thin-film field-effect transistor.

The electrostatics of the device is modeled within a top-of-the-barrier approximation [25]. Accordingly, the dependence of the potential ψ at the channel peak (i.e., the top of the channel barrier) on the gate voltage is described by means of the geometrical capacitance per unit area between the gate and the channel $C_{\mathrm{ox}} = \epsilon_0\epsilon_{\mathrm{ox}}/t_{\mathrm{ox}}$, where ϵ_0 is the vacuum permittivity, and t_{ox} can also be corrected in order to include the effects of quantum confinement in the channel. The energy E_{C} of the bottom of the lowest two-dimensional subband in the channel peak can be expressed as [26]

$$E_{\mathrm{C}} = -q(\psi + V_{\mathrm{FB}}) = -qV_{\mathrm{GS}} + \frac{qn_{\mathrm{s}}}{C_{\mathrm{ox}}}, \tag{2}$$

where n_{s} is the electron density per unit area at the channel peak, V_{GS} is the voltage applied between gate and source, and V_{FB} is the flat-band voltage. The previous equation assumes that the capacitances associated to the source and drain contacts are negligible with respect to the geometrical gate capacitance, i.e., that ψ does not depend on the drain voltage.

The electron density is computed by combining the carrier fluxes coming from the source and drain contacts, according to the formula [27]:

$$n_{\mathrm{s}} = \frac{q}{2}\int_{-\infty}^{\infty} dE\, D_{2\mathrm{D}}\, \Theta(E - E_{\mathrm{C}})\, [(2 - \mathcal{T}) f_{\mathrm{S}} + \mathcal{T} f_{\mathrm{D}}]\,, \tag{3}$$

where $\mathcal{T}$ is the transmission probability of electrons over the channel barrier, $\Theta(E)$ is the Heaviside function. the Fermi-Dirac distributions of the source and drain contacts are f_{S} and f_{D}, respectively, defined as

$$f_{\mathrm{S}} = f\,(E - E_{\mathrm{FS}}) \tag{4}$$

$$f_{\mathrm{D}} = f\,(E - E_{\mathrm{FS}} + qV_{\mathrm{DS}}), \tag{5}$$

where E_{FS} is the Fermi level of the source contact, V_{DS} is the voltage applied between the drain and source contacts, and $f(E) = 1/(1 + e^{-E/kT})$.

Under the assumption of elastic transport, the current is computed by means of the Landauer formula [27],

$$I = \frac{q}{\pi\hbar}\int_{-\infty}^{\infty} dE\, M(E)(f_{\mathrm{S}} - f_{\mathrm{D}})\mathcal{T}, \tag{6}$$

where $\mathcal{T}$ is the transmission probability in the channel, $M(E)$ the number of modes in the channel at energy E and is independent of the band profile in the channel. In the case in which a parabolic band approximation is used in the channel, $M(E)$ reduces to [27]

$$M(E) = W\frac{\pi\hbar}{2}\langle v_x\rangle D_{2D}\,\Theta(E - E_C), \tag{7}$$

where D_{2D} is the 2D density of states and $\langle v_x\rangle$ is the average injection velocity of electrons along the transport direction, given by

$$D_{2D} = g_v\frac{m^*}{\pi\hbar^2}, \langle v_x\rangle = \frac{2}{\pi}\sqrt{\frac{2(E - E_C)}{m^*}}, \tag{8}$$

where $g_v = 1$ is the valley degeneracy, m^* is the isotropic effective mass, and $\hbar$ the reduced Planck constant.

The transmission probability is assumed of the form [25]

$$\mathcal{T} = \frac{\langle\lambda\rangle}{\langle\lambda\rangle + l_c}, \tag{9}$$

where $\langle\lambda\rangle$ is the mean free path averaged over direction and energy [28], and l_c is the so-called critical length, which accounts for the dependence of the effective width of the barrier on V_{GS} and V_{DS} [29]. For further details on the derivation of the model, the reader is referred to Refs. [23,28].

III. SHOT-NOISE MODEL

First we introduce the concept of shot-noise power spectral density, S, and how it is related to the mean current, I. Let us start from the general expression of Eq. (6) and for now we do not consider the particular assumptions of our model regarding the mode distributions, transmission, etc. We rewrite the equation considering the individual transport modes, i.e., as a sum running on energy and—for each energy—as a sum on the corresponding transversal modes:

$$I = \lim_{\Delta E\to 0}\frac{q\Delta E}{\pi\hbar}\sum_{i=-\infty}^{+\infty}\sum_{j=1}^{M(E_i,E_C)} T_{ij}\,(f_{S,i} - f_{D,i}), \tag{10}$$

where $E_i = i\Delta E$. We note that Eq. (10) can be rewritten as

$$I = \lim_{\tau\to\infty}\frac{q}{\tau}N, \tag{11}$$

where N is the mean number of carriers passing through the transistor in a time interval $\tau \equiv \pi\hbar/\Delta E$. Furthermore, current fluctuations can be expressed in terms of fluctuations in the number of electrons:

$$\delta I = \lim_{\tau\to\infty}\frac{q}{\tau}\delta N, \tag{12}$$

where with "$\delta\zeta$" we denotes the fluctuation of the generical quantity "ζ," i.e., the variations with respect to the average. Following the derivation proposed by Van Der Ziel [30], we can express the shot-noise power spectral density at zero frequency as

$$\begin{aligned} S &= 2qI\frac{\text{var}(\delta N)}{N} \\ &= 2qI\frac{\text{var}\left[\delta\sum_{i=-\infty}^{+\infty}\sum_{j=1}^{M(E_i,E_C)} T_{ij}\,(f_{S,i} - f_{D,i})\right]}{\sum_{i=-\infty}^{+\infty}\sum_{j=1}^{M(E_i,E_C)} T_{ij}\,(f_{S,i} - f_{D,i})}, \end{aligned} \tag{13}$$

where var() denotes the variance. Finally, we return to the integral formulation of the equations. In doing so, let us assume that the occupation factors of different modes are uncorrelated. This implies that the variance of the energy series that we see in Eq. (13) becomes the series of variances. The final expression reads

$$S = 2qI\frac{\int_{-\infty}^{\infty} dE\, M(E)\cdot\text{var}\left[\delta(\mathcal{T}f_S - \mathcal{T}f_D)\right]}{\int_{-\infty}^{\infty} dE\, M(E)\cdot\mathcal{T}(f_S - f_D)}. \tag{14}$$

A. Shot noise in the absence of electrostatic interaction

We can first consider the case in which we do not take into account the fluctuations of the electrostatic potential, i.e., $\mathcal{T}$ is independent of the occupation of modes in the channel. Let us denote by I_0 the corresponding current and by S_0 the noise spectral density. This is the case of the well-known result first obtained by Lesovik [31] and generalized by Büttiker [32], and predicts a Fano factor always smaller than unity due to Pauli exclusion.

From Eqs. (6)–(8), considering parabolic bands, we obtain

$$\delta I_0 = \alpha\int_0^{\infty} d\eta\,\sqrt{\eta}\,\delta[\mathcal{T}f_S - \mathcal{T}f_D]. \tag{15}$$

We have defined $\alpha \equiv qWv_TkTD_{2D}/\sqrt{\pi}$ and $\eta \equiv (E - E_C)/kT$, where $v_T = \sqrt{2kT/q\pi m^*}$ is the thermal velocity. From Eq. (14) we can obtain the current noise power spectral density at zero frequency S_0 in the famous work by Markus Büttiker [32]:

$$\begin{aligned} S_0 &= 2q\alpha\int_0^{\infty} d\eta\,\sqrt{\eta}\,\text{var}\left[\delta\left(\mathcal{T}f_S - \mathcal{T}f_D\right)\right] \\ &= 2q\alpha\int_0^{\infty} d\eta\,\sqrt{\eta}\left[\mathcal{T}f_S(1 - f_S) + \mathcal{T}f_D(1 - f_D)\right. \\ &\quad \left. + \mathcal{T}(1 - \mathcal{T})(f_S - f_D)^2\right], \end{aligned} \tag{16}$$

According to Eq. (16), a Poissonian regime is approached only for $f_S, f_D \ll 1$, namely when the correlations induced by the Pauli exclusion principle are negligible and the electron distribution approximately follows the Maxwell-Boltzmann statistics.

B. Shot noise in the presence of electrostatic interaction

We introduce the electrostatic fluctuations following Ref. [7]. Here, we also take into account that the transmission probability is not either zero or one, as assumed in the purely ballistic model of Ref. [7]. When the electrostatic potential fluctuations are taken into account, δI becomes

$$\delta I = \alpha \int_0^\infty d\eta\, \sqrt{\eta}\, \delta[\mathcal{T} f_{\mathrm{S}} - \mathcal{T} f_{\mathrm{D}}] + \alpha\, \delta E_{\mathrm{C}} \int_0^\infty d\eta\, \sqrt{\eta}\, \frac{\partial[\mathcal{T} f_{\mathrm{S}} - \mathcal{T} f_{\mathrm{D}}]}{\partial E_{\mathrm{C}}}. \tag{17}$$

From Eqs. (2) and (3), we can relate δE_{C} to the fluctuation of the carrier density δn_{s} as

$$\delta E_{\mathrm{C}} = \frac{q}{C_{ox}}\, \delta n_s, \tag{18}$$

where δn_s can be computed from Eq. (3) as

$$\delta n_{\mathrm{s}} = \beta \int_0^\infty d\eta\, \delta[(2 - \mathcal{T}) f_{\mathrm{S}} + \mathcal{T} f_{\mathrm{D}}] + \beta\, \delta E_{\mathrm{C}} \int_0^\infty d\eta\, \frac{\partial[(2 - \mathcal{T}) f_{\mathrm{S}} + \mathcal{T} f_{\mathrm{D}}]}{\partial E_{\mathrm{C}}}, \tag{19}$$

where $\beta = qkTD_{2\mathrm{D}}/2$. From Eqs. (18) and (19), we obtain

$$\delta E_{\mathrm{C}} = \frac{\beta \int_0^\infty d\eta\, \delta[(2 - \mathcal{T}) f_{\mathrm{S}} + \mathcal{T} f_{\mathrm{D}}]}{C_{\mathrm{ox}} - \beta \int_0^\infty d\eta\, \frac{\partial[(2-\mathcal{T}) f_{\mathrm{S}} + \mathcal{T} f_{\mathrm{D}}]}{\partial E_{\mathrm{C}}}}, \tag{20}$$

which, replaced in Eq. (17) and after rearranging, results in

$$\delta I = \alpha \int_0^\infty d\eta\, \sqrt{\eta}\, \delta\Big[\mathcal{T}(f_{\mathrm{S}} - f_{\mathrm{D}}) + \gamma (f_{\mathrm{S}} + f_{\mathrm{D}}) + \gamma (1 - \mathcal{T})(f_{\mathrm{S}} - f_{\mathrm{D}})\Big]. \tag{21}$$

In the previous equation, γ collects the terms that do not fluctuate, and is defined by

$$\gamma = \frac{1}{\sqrt{\eta}}\, \frac{\beta \int_0^\infty d\eta\, \sqrt{\eta}\, \frac{\partial[\mathcal{T} f_{\mathrm{S}} - \mathcal{T} f_{\mathrm{D}}]}{\partial E_{\mathrm{C}}}}{C_{\mathrm{ox}} - \beta \int_0^\infty d\eta\, \frac{\partial[(2-\mathcal{T}) f_{\mathrm{S}} + \mathcal{T} f_{\mathrm{D}}]}{\partial E_{\mathrm{C}}}}. \tag{22}$$

Equation (21) allows us to compute the total power spectral density S. The detailed derivation is reported in the Appendix: we find that S can be written as the sum of three

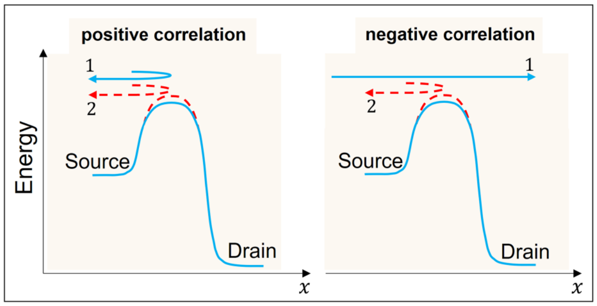

FIG. 2. Illustration of positive and negative correlation between the motion of two electrons injected by the source contact. When electron 1 impinges on the barrier, the latter rises (dashed red curve) entailing a higher reflection probability for the subsequent electron 2. If electron 1 is reflected, the motion directions of the two electrons tend to be positively correlated. Otherwise, a negative correlation tends to be established.

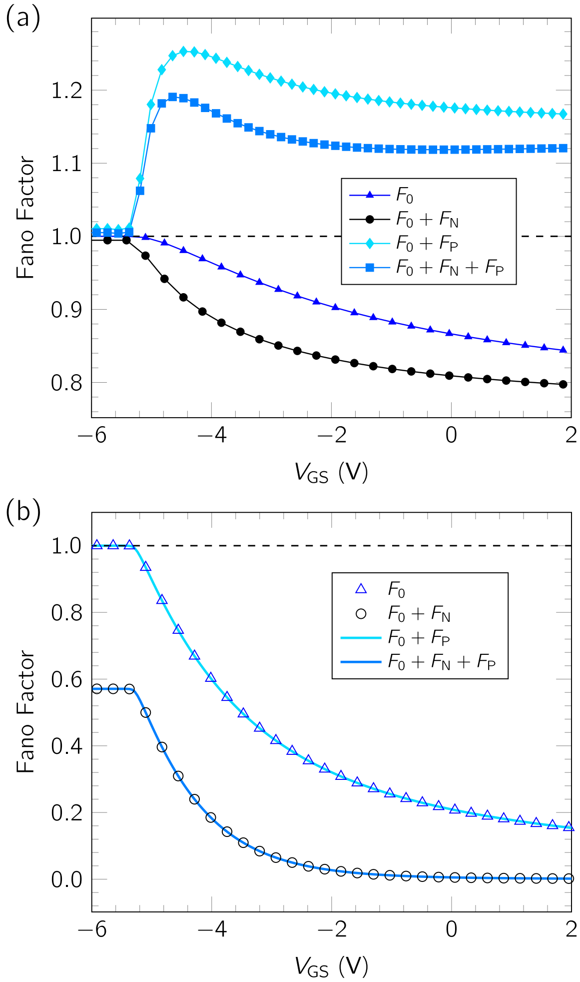

FIG. 3. (a) Total Fano factor and some representative partial sums of the contributions F_0, F_{N}, and F_{P}. (b) Same as panel (a), but enforcing $\mathcal{T} = 1$.

terms:

$$S = S_0 + S_{\mathrm{N}} + S_{\mathrm{P}}, \tag{23}$$

where S_0 is provided in Eq. (16), and the terms S_{N} and S_{P} account for the fluctuation of the electrostatic potential and have the following expressions:

$$S_{\mathrm{N}} \equiv 2q\alpha \int_0^\infty d\eta \sqrt{\eta} \Big[\big(\gamma^2 + 2\gamma \mathcal{T}\big) f_{\mathrm{S}}(1-f_{\mathrm{S}}) + \big(\gamma^2 - 2\gamma \mathcal{T}\big) f_{\mathrm{D}}(1-f_{\mathrm{D}}) \Big], \tag{24}$$

$$S_{\mathrm{P}} \equiv 2q\alpha \int_0^\infty d\eta \sqrt{\eta}(1-\mathcal{T}) \Big[3\gamma^2 f_{\mathrm{S}}(1-f_{\mathrm{S}}) - \gamma^2 f_{\mathrm{D}}(1-f_{\mathrm{D}}) + \big(\gamma^2 - 2\gamma\big) \mathcal{T} (f_{\mathrm{S}} - f_{\mathrm{D}})^2 \Big]. \tag{25}$$

In order to discuss an intuitive physical interpretation of S_{N} and S_{P}, we refer to the transport picture in Fig. 2. When an electron (1) impinges on the potential barrier in the channel, a subsequent electron (2) sees a higher potential barrier, due to electrostatic repulsion, and therefore experiences a higher reflection probability. However, the sign of the correlation of the motion of the two electrons depends on the fact that the first electron is actually transmitted or backscattered. There are two cases:

(1) If the first electron is transmitted (Fig. 2, right), the fluctuation of the barrier induces a negative correlation with the next electron.

(2) If the first electron is backscattered (Fig. 2, left), the fluctuation of the barrier positively correlates the motion of the electrons.

In a high-transmission regime, when events of the former case are more probable, negative correlations are more common and we should expect sub-Poissonian shot noise. In a low-transmission regime, when events of the latter case are more probable, positive correlations are more common and we should expect super-Poissonian shot noise.

Considering Eqs. (24) and (25), we notice that S_{P} vanishes for $\mathcal{T}$ approaching 1, which corresponds to the situation in which the electron motion tends to be always negatively correlated. In these conditions, only the term S_{N} survives. We can therefore interpret S_{N} as originating uniquely from *negative* correlations, while tracing back S_{P} to the *positive* ones. Our simulations corroborate this hypothesis, since S_{N} and S_{P} show a definite and opposite sign: the former is always lesser or equal to zero, while the latter is always greater or equal to zero.

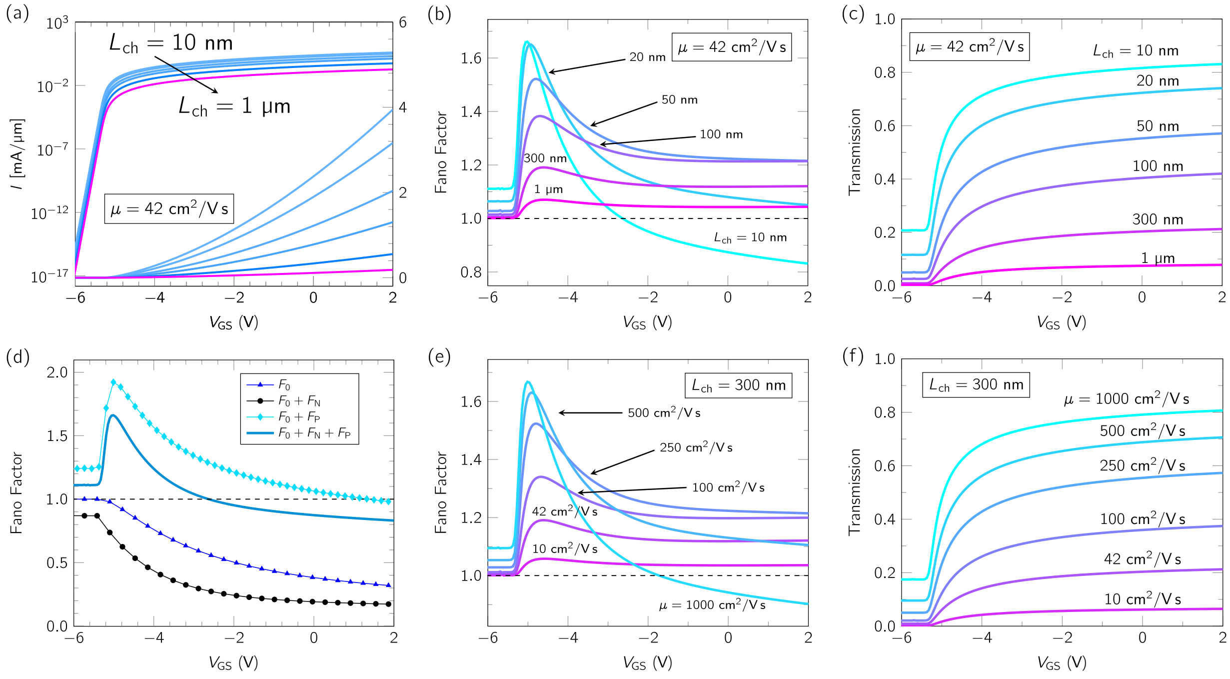

FIG. 4. (a) Fano factor as a function of V_{GS} for different channel lengths L_{ch}. (b) Transmission $\mathcal{T}$ as a function of V_{GS} for different values of L_{ch}. (c) Transfer characteristics $I - V_{\mathrm{GS}}$ as a function of V_{GS} for different channel lengths L_{ch}. (d) Fano factor for $L_{\mathrm{ch}} = 10$ nm together with some representative partial sums of the different contributions F_0, F_N, and F_P. (e) Fano factor as a function of V_{GS} for different values of the channel mobility μ. (f) Transmission $\mathcal{T}$ as a function of V_{GS} for different values of μ. In all figures $V_{\mathrm{DS}} = 1$ V.

According to Eq. (23), the Fano factor can be expanded as the sum of three contributions:

$$F = F_0 + F_{\mathrm{N}} + F_{\mathrm{P}}, \tag{26}$$

where

$$F_0 = \frac{S_0}{2qI}, \quad F_{\mathrm{N}} = \frac{S_{\mathrm{N}}}{2qI}, \quad F_{\mathrm{P}} = \frac{S_{\mathrm{P}}}{2qI}.$$

IV. CASE OF A CONDUCTIVE OXIDE THIN-FILM FET

Without loss of generality, we first consider a conductive oxide thin-film FET, the same for which the presented transistor model has been derived [23,33]. The channel material is La-BaSnO$_3$ with $m^* = 0.42\ m_0$ and electron mobility $\mu = 42$ cm^2 V^{-1} s^{-1}; $V_{\mathrm{DS}} = 1$ V. Other simulation parameters are $L_{\mathrm{ch}} \simeq 300$ nm, $W \simeq 1$ μm, $t_{\mathrm{ox}} = 23$ nm;

Figure 3(a) shows the Fano factor in the transistor as a function of V_{GS}. To clearly illustrate the effect of each contribution, F_0, $F_0 + F_{\mathrm{N}}$, and $F_0 + F_{\mathrm{P}}$ are also shown. In agreement with the previous discussion, the plot highlights that the terms F_0 and F_{N} are associated to a suppression of the Fano factor, while the term F_{P} tends to enhance it above unity. The overall behavior of F depends on the relative weight of the single contributions. In this respect, it is useful to compare the case of Fig. 3(a), where F_{P} dominates, with that in Fig. 3(b), obtained by purposely setting $\mathcal{T} = 1$ for $E > E_C$ and for any V_{GS}. In this condition, $F_{\mathrm{P}} = 0$ and the Fano factor is always suppressed.

A. Dependence on the device parameters

As observed in the previous section, an increase in the transmission probability through the channel can lead to a transition of the Fano factor from enhancement to suppression. To explore further the possibility of a crossover between super-Poissonian and sub-Poissonian regime as the gate voltage is varied, we investigate the dependence of the Fano factor on the physical and geometrical parameters of the transistor.

Figures 4(a) and 4(b) show the transfer characteristics of the device and the Fano factor as a function of V_{GS} for different channel lengths in the range from $L_{\mathrm{ch}} = 10$ nm to $L_{\mathrm{ch}} = 1$ μm. The Fano factor exhibits a super-Poissonian peak at gate voltages close to the threshold voltage, which becomes higher and narrower as L_{ch} decreases. Moreover, for $L_{\mathrm{ch}} = 10$ nm a transition from super-Poissonian to sub-Poissonian regime is clearly visible at $V_{\mathrm{GS}} \approx -2.65$ V. This behavior can be explained with the help of panels (c) and (d) of Fig. 4.

The former reports the transmission as a function of V_{GS} and L_{ch} and shows that it is an increasing function of V_{GS} and a decreasing function of L_{ch}. Figure 4(d) resolves the Fano factor for $L_{\mathrm{ch}} = 10$ nm into the sum of different contributions. The Fano factor peak originates from the competition between the term $F_0 + F_{\mathrm{N}}$, which decreases as $\mathcal{T}$ increases, and F_{P}, which has a sudden increase as V_{GS} reaches the threshold voltage [see Fig. 4(d)]. For $L_{\mathrm{ch}} = 10$ nm, $\mathcal{T}$ reaches large enough values on the considered V_{GS} range to sufficiently suppress F_{P} and induce the crossover between super- and sub-Poissonian regimes.

The same considerations apply to Fig. 4(e), that reports the Fano factor as a function of V_{GS} for channel mobility in the range from $\mu = 10$ cm^2 V^{-1} s^{-1} to $\mu = 1000$ cm^2 V^{-1} s^{-1}. As shown in Fig. 4(f), the transmission is an increasing function of μ and a crossover between the super- and sub-Poissonian regimes is observed for $\mu = 1000$ cm^2 V^{-1} s^{-1}.

The influence of the bias voltage V_{DS} is explored in Figs. 5(a) and 5(b), that compare the results obtained for $V_{\mathrm{DS}} = 1$ V and $V_{\mathrm{DS}} = 4$ V. Figure 5(b) shows that increasing V_{DS} entails a systematic increase of the transmission at each V_{GS}. This behavior results from a decrease of the critical length l_c [28], which, according to Eq. (9),

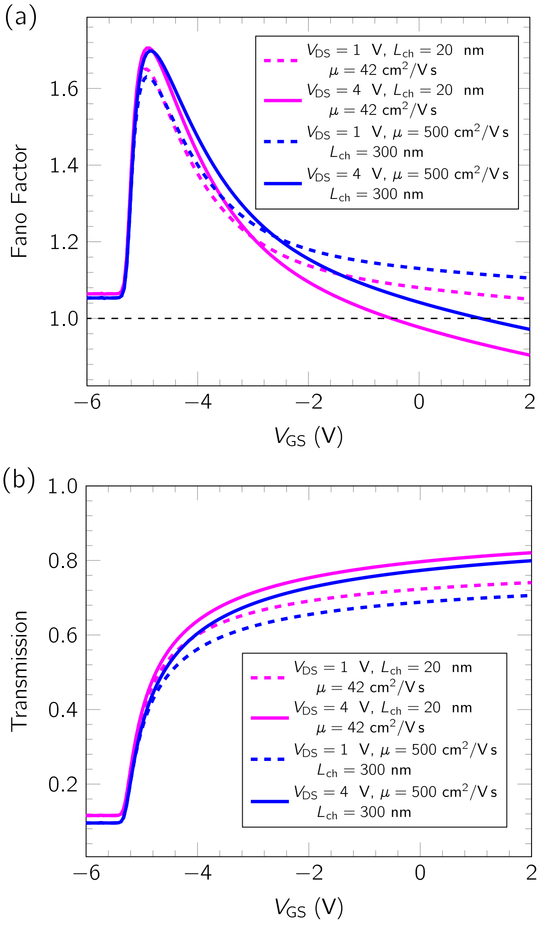

FIG. 5. (a) Fano factor as a function of V_{GS} at $L_{\mathrm{ch}} = 20$ nm and at $\mu = 500$ cm^2 V^{-1} s^{-1}, for different values of V_{DS}. (b) Transmission $\mathcal{T}$ as a function of V_{GS} for the same sets of parameters as in (a).

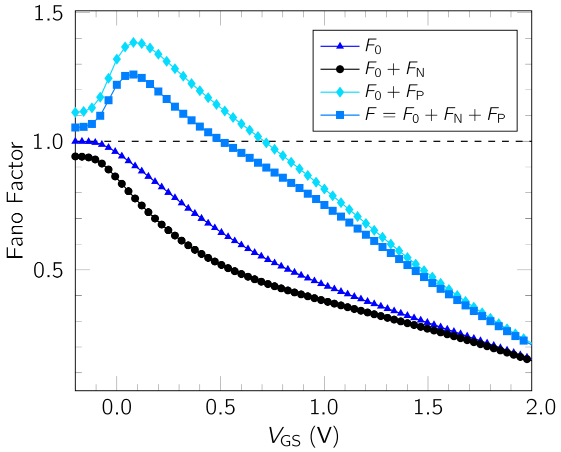

FIG. 6. Total Fano factor and the representative partial sums of the contributions, F_0, F_N, and F_P, as a function of V_{GS}, for $V_{DS} = 0.5$ V.

translates to an increase of the transmission. As a consequence, the crossover between the two noise regimes can be observed at larger L_{ch} and lower mobilities.

V. CASE OF A SILICON METAL-OXIDE-SEMICONDUCTOR FET

In order to check whether this behavior can be observed also in a standard silicon metal-oxide-semiconductor FET (MOSFET), we simulated the Fano factor in the 130-nm complementary MOS technology. In order to take into account quantum confinement effects, electrons in the transistor channel were modeled as a two-dimensional gas with isotropic effective mass [34]. The self-consistent model adopted is essentially identical to the one described in Sec. II. We consider the following device parameters, typical for a 130-nm process: $L_{ch} = 120$ nm, $W = 10$ µm, $t_{ox} = 2$ nm; the effective mass is $m^* = 0.19\, m_0$, the electron mobility $\mu = 300$ cm^2 V^{-1} s^{-1}, $R_C = 100\ \Omega$ µm.

To obtain results more directly comparable to measurements, the contribution of the thermal noise due to the contact resistances has been included in the spectral density used to compute the Fano factor.

Figure 6 shows the behavior of the Fano factor as a function of V_{GS} as well as the different contributions F_0, F_N, and F_P. While the effect of the thermal noise associated to the contact resistances is expected to weaken and partly hide the super-Poissonian noise, our simulations suggest that a crossover between super- and sub-Poissonian regimes can be observed.

VI. CONCLUSION

We investigated shot noise in field-effect transistors, considering the correlations induced by the interplay between a finite backscattering probability in the channel and electrostatic interaction among carriers.

We have proposed a mechanism that is additional to the effect of Pauli exclusion [31,32] and the effect of electrostatic interaction due to fluctuations in mode occupation [17]. Remarkably, this effect can lead to an enhancement of shot noise, that should be observed also at room temperature in conventional MOSFETs, in conditions of subthreshold or weak inversion operation and if contact resistances are sufficiently small.

Let us highlight the fact that the approximations introduced by our transport model serve the purpose of obtaining simple expressions, but do not limit our conclusions. For example, in the case of tunneling or of nonparabolic band structure, we expect a different expression for the transmission probability, that however does not affect our physical insight and the observation of the proposed effect. Analogously, a large contact resistance would multiply the noise spectral density by a partition factor smaller than one, leading to a Fano factor below unity, however we believe the signature peak of the Fano factor in subthreshold conditions shown in Fig. 6 would still be observed. The effect of contact resistance can also be removed by using four-probe measurement techniques [35]. Finally, we do not expect phonons to influence the presence of the crossover, since the super-Poissonian regime is particularly evident in the subthreshold operation region, when electron-phonon scattering is negligible.

ACKNOWLEDGMENTS

This research has been supported by the CHARM project from the ECSEL Joint Undertaking (Grant Agreement No. 876362) and by the ForeLab funded by the Italian Ministry of Education under the programme “Dipartimenti di Eccellenza.”

APPENDIX

In order to evaluate the power spectral density S of the current noise, we need to calculate the variance of the argument of the integral in Eq. (21). We find

$$\begin{aligned} S &= 2q\alpha \int_0^\infty d\eta\, \sqrt{\eta}\, \mathrm{var}\Big[\delta\Big[\mathcal{T}(f_S - f_D) + \gamma(f_S + f_D) + \gamma(1-\mathcal{T})(f_S - f_D)\Big]\Big] \\ &= 2q\alpha \int_0^\infty d\eta\, \sqrt{\eta}\, \mathrm{var}(P_0 + P_N + P_P), \end{aligned} \tag{A1}$$

where

$$\begin{aligned} P_0 &\equiv \delta[\mathcal{T}(f_\mathrm{S}-f_\mathrm{D})],\\ P_\mathrm{N} &\equiv \gamma\delta[(f_\mathrm{S}+f_\mathrm{D})],\\ P_\mathrm{P} &\equiv \gamma\delta[(1-\mathcal{T})(f_\mathrm{S}-f_\mathrm{D})]. \end{aligned} \tag{A2}$$

The rightmost side of Eq. (A1) can be developed as

$$\begin{aligned} &2q\alpha\int_0^\infty d\eta\,\sqrt{\eta}\,\mathrm{var}(P_0+P_\mathrm{N}+P_\mathrm{P}) =\\ &= 2q\alpha\int_0^\infty d\eta\,\sqrt{\eta}\,\Big[\mathrm{var}(P_\mathrm{P})+\mathrm{var}(P_\mathrm{N})+\mathrm{var}(P_0)+2\,\mathrm{cov}(P_\mathrm{P},P_\mathrm{N})+2\,\mathrm{cov}(P_\mathrm{P},P_0)+2\,\mathrm{cov}(P_\mathrm{N},P_0)\Big]\\ &= S_0+S_\mathrm{N}+S_\mathrm{P}, \end{aligned} \tag{A3}$$

where var() denotes the variance, cov() the covariance and

$$\begin{aligned} S_0 &\equiv 2q\alpha\int_0^\infty d\eta\,\sqrt{\eta}\,\mathrm{var}(P_0),\\ S_\mathrm{N} &\equiv 2q\alpha\int_0^\infty d\eta\,\sqrt{\eta}\,\Big[\mathrm{var}(P_\mathrm{N})+2\,\mathrm{cov}(P_0,P_\mathrm{N})\Big],\\ S_\mathrm{P} &\equiv 2q\alpha\int_0^\infty d\eta\,\sqrt{\eta}\,\Big[\mathrm{var}(P_\mathrm{P})+2\,\mathrm{cov}(P_\mathrm{P},P_0)+2\,\mathrm{cov}(P_\mathrm{P},P_\mathrm{N})\Big]. \end{aligned} \tag{A4}$$

S_0 is the shot-noise spectral density obtained when Coulomb interactions are disregarded. Its expression in Eq. (A2) directly leads to Eq. (16) of the main text. S_P is the sum of all the terms involving a $1-\mathcal{T}$ factor, and therefore vanishing for $\mathcal{T}$ approaching unity. Finally, S_N is the sum of all the remaining terms.

The expressions of S_N and S_P in Eq. (A4) can be further developed as follows:

$$\begin{aligned} S_\mathrm{N} &= 2q\alpha\int_0^\infty d\eta\,\sqrt{\eta}\,\Big[\mathrm{var}(P_\mathrm{N})+2\,\mathrm{cov}(P_0,P_\mathrm{N})\Big]\\ &= 2q\alpha\int_0^\infty d\eta\,\sqrt{\eta}\,\Big\{\mathrm{var}\big[\gamma(f_\mathrm{S}+f_\mathrm{D})\big]+2\,\mathrm{cov}\big[\mathcal{T}(f_\mathrm{S}-f_\mathrm{D}),\gamma(f_\mathrm{S}+f_\mathrm{D})\big]\Big\}\\ &= 2q\alpha\int_0^\infty d\eta\,\sqrt{\eta}\,\Big\{\gamma^2\big[\mathrm{var}(f_\mathrm{S})+\mathrm{var}(f_\mathrm{D})+2\,\mathrm{cov}(f_\mathrm{S},f_\mathrm{D})\big]\\ &\quad+\;2\gamma\Big[\mathrm{cov}\big[\mathcal{T}f_\mathrm{S},f_\mathrm{S}\big]+\mathrm{cov}\big[\mathcal{T}f_\mathrm{S},f_\mathrm{D}\big]-\mathrm{cov}\big[\mathcal{T}f_\mathrm{D},f_\mathrm{S}\big]-\mathrm{cov}\big[\mathcal{T}f_\mathrm{D},f_\mathrm{D}\big]\Big]\Big\}\\ &= 2q\alpha\int_0^\infty d\eta\,\sqrt{\eta}\,\Big[\gamma^2\big[f_\mathrm{S}(1-f_\mathrm{S})+f_\mathrm{D}(1-f_\mathrm{D})\big]+\;2\gamma\mathcal{T}\big[f_\mathrm{S}(1-f_\mathrm{S})-f_\mathrm{D}(1-f_\mathrm{D})\big]\Big], \end{aligned} \tag{A5}$$

$$\begin{aligned} S_\mathrm{P} &= 2q\alpha\int_0^\infty d\eta\,\sqrt{\eta}\,\big[\mathrm{var}(P_\mathrm{P})+2\,\mathrm{cov}(P_\mathrm{P},P_0)+2\,\mathrm{cov}(P_\mathrm{P},P_\mathrm{N})\big]\\ &= 2q\alpha\int_0^\infty d\eta\,\sqrt{\eta}\,\Big[\mathrm{var}\big[\gamma(1-\mathcal{T})(f_\mathrm{S}-f_\mathrm{D})\big]+2\,\mathrm{cov}\big[\gamma(1-\mathcal{T})(f_\mathrm{S}-f_\mathrm{D}),\mathcal{T}(f_\mathrm{S}-f_\mathrm{D})\big]\\ &\quad+\;2\,\mathrm{cov}\big[\gamma(1-\mathcal{T})(f_\mathrm{S}-f_\mathrm{D}),\gamma(f_\mathrm{S}+f_\mathrm{D})\big]\Big]\\ &= 2q\alpha\int_0^\infty d\eta\,\sqrt{\eta}\,\Big\{\gamma^2\Big[\mathrm{var}\big[(1-\mathcal{T})f_\mathrm{S}\big]+\mathrm{var}\big[(1-\mathcal{T})f_\mathrm{D}\big]-2\,\mathrm{cov}\big[(1-\mathcal{T})f_\mathrm{S},(1-\mathcal{T})f_\mathrm{D}\big]\Big] \end{aligned} \tag{A6}$$

$$
\begin{aligned}
&+2\gamma\Big[\mathrm{cov}\big[\mathcal{T}f_{\mathrm{S}},(1-\mathcal{T})f_{\mathrm{S}})\big]-\mathrm{cov}\big[\mathcal{T}f_{\mathrm{S}},(1-\mathcal{T})f_{\mathrm{D}}\big]+\mathrm{cov}\big[\mathcal{T}f_{\mathrm{D}},(1-\mathcal{T})f_{\mathrm{D}}\big]-\mathrm{cov}\big[\mathcal{T}f_{\mathrm{D}},(1-\mathcal{T})f_{\mathrm{S}}\big]\Big]\\
&+\ 2\gamma^2\Big[\mathrm{cov}\big[f_{\mathrm{S}},(1-\mathcal{T})f_{\mathrm{S}}\big]-\mathrm{cov}\big[f_{\mathrm{S}},(1-\mathcal{T})f_{\mathrm{D}}\big]+\mathrm{cov}\big[f_{\mathrm{D}},(1-\mathcal{T})f_{\mathrm{S}}\big]-\mathrm{cov}\big[f_{\mathrm{D}},(1-\mathcal{T})f_{\mathrm{D}}\big]\Big]\Big\}\\
&=2q\alpha\int_0^\infty d\eta\,\sqrt{\eta}\,\Big\{\gamma^2\Big[(1-\mathcal{T})(f_{\mathrm{S}}(1-f_{\mathrm{S}})+(1-\mathcal{T})(f_{\mathrm{D}}(1-f_{\mathrm{D}})+\mathcal{T}(1-\mathcal{T})(f_{\mathrm{S}}-f_{\mathrm{D}})^2\Big]+\\
&-2\gamma\mathcal{T}(1-\mathcal{T})(f_{\mathrm{S}}-f_{\mathrm{D}})^2+2\gamma^2(1-\mathcal{T})\Big[f_{\mathrm{S}}(1-f_{\mathrm{S}})-f_{\mathrm{D}}(1-f_{\mathrm{D}})\Big]\Big\},
\end{aligned}
\tag{A7}
$$

where in both equations we have dropped all the terms proportional to the covariance between independent variables.

After rearranging the terms, the final expressions in Eqs. (A5) and (A6) coincide with the left side of Eqs. (24) and (25) of the main text.

1. Thermal noise limit

Let us consider the limit of Eq. (23) as the system approaches equilibrium conditions, namely for $V_{\mathrm{DS}} \to 0$. In this limit, $f_{\mathrm{S}} \simeq f_{\mathrm{D}} \equiv f$, γ vanishes and the power spectral density becomes

$$
S \to 4\,kT\,\frac{q^2 W v_{\mathrm{T}} D_{2\mathrm{D}}}{2\sqrt{\pi}}\int_0^\infty d\eta\,\sqrt{\eta}\,\times\Big[2\,\mathcal{T}f\,(1-f\,)\Big]=4kTG_{\mathrm{eq}},
\tag{A8}
$$

where

$$
G_{\mathrm{eq}}=\lim_{V_{\mathrm{DS}}\to 0}\frac{\partial I}{\partial V_{\mathrm{DS}}}=\frac{q^2 W v_{\mathrm{T}} D_{2\mathrm{D}}}{2\sqrt{\pi}}\int_0^\infty d\eta\,\sqrt{\eta}\Big[2\,\mathcal{T}f\,(1-f\,)\Big]
$$

is the differential conductance of the transistor channel for $V_{\mathrm{DS}} \to 0$. Therefore, at equilibrium, S correctly reduces to the thermal noise power spectral density [36].

[1] Rolf Landauer, The noise is the signal, Nature **392**, 658 (1998).

[2] G. Iannaccone, M. Macucci, and B. Pellegrini, Shot noise in resonant-tunneling structures, Phys. Rev. B **55**, 4539 (1997).

[3] G. Iannaccone, G. Lombardi, M. Macucci, and B. Pellegrini, Enhanced shot noise in resonant tunneling: Theory and experiment, Phys. Rev. Lett. **80**, 1054 (1998).

[4] Ya. M. Blanter and M. Büttiker, Shot-noise current-current correlations in multiterminal diffusive conductors, Phys. Rev. B **56**, 2127 (1997).

[5] R. J. Schoelkopf, P. J. Burke, A. A. Kozhevnikov, D. E. Prober, and M. J. Rooks, Frequency dependence of shot noise in a diffusive mesoscopic conductor, Phys. Rev. Lett. **78**, 3370 (1997).

[6] Eugene V. Sukhorukov and Daniel Loss, Universality of shot noise in multiterminal diffusive conductors, Phys. Rev. Lett. **80**, 4959 (1998).

[7] G. Iannaccone, Analytical and numerical investigation of noise in nanoscale ballistic field effect transistors, J. Comput. Electron. **3**, 199 (2004).

[8] J. Jeon, J. Lee, J. Kim, C. H. Park, H. Lee, H. Oh, H.-K. Kang, B.-G. Park, and H. Shin, in *2009 Symposium on VLSI Technology* (IEEE, Kyoto, Japan, 2009), p. 48.

[9] C. Spathis, A. Birbas, and K. Georgakopoulou, Semi-classical noise investigation for sub-40 nm metal-oxide-semiconductor field-effect transistors, AIP Adv. **5**, 087114 (2015).

[10] G. Iannaccone, F. Crupi, B. Neri, and S. Lombardo, Theory and experiment of suppressed shot noise in 'stress-induced leakage currents, IEEE Trans. Electron Devices **50**, 1363 (2003).

[11] Jonghwan Lee, Unified model of shot noise in the tunneling current in sub-10 nm MOSFETs, Nanomaterials **11**, 2759 (2021).

[12] Giuseppe Iannaccone, Alessandro Betti, and Gianluca Fiori, Suppressed and enhanced shot noise in one dimensional field-effect transistors, J. Comput. Electron. **14**, 94 (2015).

[13] L. DiCarlo, J. R. Williams, Yiming Zhang, D. T. McClure, and C. M. Marcus, Shot noise in graphene, Phys. Rev. Lett. **100**, 156801 (2008).

[14] A. Betti, G. Fiori, and G. Iannaccone, in *2008 IEEE International Electron Devices Meeting* (IEEE, San Francisco, CA, USA, 2008), p. 1.

[15] Alessandro Betti, Gianluca Fiori, and Giuseppe Iannaccone, Statistical theory of shot noise in quasi-one-dimensional field-effect transistors in the presence of electron-electron interaction, Phys. Rev. B **81**, 035329 (2010).

[16] A. Betti, G. Fiori, and G. Iannaccone, in *2010 14th International Workshop on Computational Electronics* (IEEE, Pisa, Italy, 2010), p. 1.

[17] Giuseppe Iannaccone, Analytical and numerical investigation of noise in nanoscale ballistic field effect transistors, J. Comput. Electron. **3**, 199 (2004).

[18] Reza Navid, Christoph Jungemann, Thomas H. Lee, and Robert W. Dutton, High-frequency noise in nanoscale metal oxide semiconductor field effect transistors, J. Appl. Phys. **101**, 124501 (2007).

[19] Xuesong Chen, Chih-Hung Chen, and Ryan Lee, Fast evaluation of the high-frequency channel noise in nanoscale MOSFETs, IEEE Trans. Electron Devices **65**, 1502 (2018).

[20] V. Ya. Aleshkin and L. Reggiani, Electron transport and shot noise in double-barrier resonant diodes: The role of Pauli and Coulomb correlations, Phys. Rev. B **64**, 245333 (2001).

[21] V. Ya. Aleshkin, L. Reggiani, and M. Rosini, Comparative analysis of sequential and coherent tunneling models in resonant diodes, Phys. Rev. B **73**, 165320 (2006).

[22] Duo Li, Lei Zhang, Fuming Xu, and Jian Wang, Enhancement of shot noise due to the fluctuation of Coulomb interaction, Phys. Rev. B **85**, 165402 (2012).

[23] Fabrizio Mazziotti, Demetrio Logoteta, and Giuseppe Iannaccone, $(\mathrm{La,Ba})\mathrm{SnO}_3$-based thin-film transistors: Large-signal model and scaling projections, Phys. Rev. Appl. **17**, 014011 (2022).

[24] John H. Davies, *The Physics of Low-Dimensional Semiconductors* (Cambridge University Press, New York, NY, USA, 1997).

[25] A. Rahman and M. S. Lundstrom, A compact scattering model for the nanoscale double-gate MOSFET, IEEE Trans. Electron Devices **49**, 481 (2002).

[26] Risho Koh, Haruo Kato, and Hiroshi Matsumoto, Capacitance network model of the short channel effect for 0.1 μm fully depleted SOI MOSFET, Jpn. J. Appl. Phys. **35**, 996 (1996).

[27] M. Lundstrom and J. Guo, *Nanoscale Transistors: Physics, Modeling, and Simulation* (Springer-Verlag, New York, NY, USA, 2006).

[28] Shaloo Rakheja, Mark Lundstrom, and Dimitri Antoniadis, in *2014 IEEE International Electron Devices Meeting* (IEEE, San Francisco, CA, USA, 2014), p. 35.1.1.

[29] Mark Lundstrom, Supriyo Datta, and Xingshu Sun, Emission-diffusion theory of the MOSFET, IEEE Trans. Electron Devices **62**, 4174 (2015).

[30] A. Van Der Ziel, Noise in junction transistors, Proc. IRE **46**, 1019 (1958).

[31] G. B. Lesovik, Excess quantum noise in 2D ballistic point contacts, JETP Lett. **49**, 592 (1989).

[32] M. Büttiker, Scattering theory of thermal and excess noise in open conductors, Phys. Rev. Lett. **65**, 2901 (1990).

[33] Jisung Park, Hanjong Paik, Kazuki Nomoto, Kiyoung Lee, Bo-Eun Park, Benjamin Grisafe, Li-Chen Wang, Sayeef Salahuddin, Suman Datta, Yongsung Kim, Debdeep Jena, Huili Grace Xing, and Darrell G. Schlom, Fully transparent field-effect transistor with high drain current and on-off ratio, APL Mater. **8**, 011110 (2020).

[34] David Esseni, Pierpaolo Palestri, and Luca Selmi, *Nanoscale MOS Transistors: Semi-Classical Transport and Applications* (Cambridge University Press, New York, NY, USA, 2011).

[35] Surajit Sutar, Inge Asselberghs, Dennis H. C. Lin, Aaron Voon-Yew Thean, and Iuliana Radu, FETs on 2-D materials: Deconvolution of the channel and contact characteristics by four-terminal resistance measurements on WSe_2 transistors, IEEE Trans. Electron Devices **64**, 2970 (2017).

[36] Rolf Landauer, Solid-state shot noise, Phys. Rev. B **47**, 16427 (1993).